The uplifted terraces of the Arkitsa region, NW Evoikos Gulf, Greece: a result of combined tectonic and volcanic processes?

Dimitris Papanastassiou[1], A. B. Cundy[2*], K. Gaki-Papanastassiou[3], M. R. Frogley[4], K. Tsanakas[3], H. Maroukian[3]

[1] Institute of Geodynamics, National Observatory of Athens, Gr 11810 Athens, Greece

[2] School of Environment and Technology, University of Brighton, Brighton, BN2 4GJ, UK

[3] Department of Geography-Climatology, University of Athens, Gr 15784 Athens, Greece

[4] Department of Geography, University of Sussex, Falmer, Brighton, BN1 9QJ, UK

* Corresponding author: School of Environment and Technology, University of Brighton, Brighton, BN2 4GJ, UK. Email: A.Cundy@brighton.ac.uk; Tel: +44 1273 642270; Fax: +44 1273 642285

ABSTRACT

The Arkitsa-Kamena Vourla area of central Greece occupies a zone of accommodation between the two tectonic provinces of the North Aegean Trough (the extension of the North Anatolian fault system) and the Gulf of Corinth, and is characterised by a series of very prominent tectonic landforms, notably the large (*ca*. 1000 m elevation) footwall ridge of the Arkitsa-Kamena Vourla fault system. Despite the highly prominent nature of this footwall ridge and the presence of very fresh tectonic landforms this fault system is not known to have hosted any major historical earthquakes, and the tectonic and geomorphic evolution of the Arkitsa-Kamena Vourla area remains poorly constrained. This paper utilises a combined geomorphological, sedimentological and macro-/micro-fossil approach to evaluate the Late Quaternary evolution of the Arkitsa area, in the eastern part of the fault system, focussing on prominent uplifted terraces present in the hangingwall of the Arkitsa fault. Three distinct raised glacio-lacustrine terraces, and previously reported uplifted marginal marine deposits, suggest sustained uplift of the coastline at a rate of 1 – 1.5 mm/y over at least the last 40,000 years, possibly to 75,000 BP. While movement on an offshore normal fault strand may explain more recent coastal uplift, purely fault-driven longer-term uplift at this rate requires anomalously high fault slip and extension rates. Consequently, the development of the terraces and other geomorphic indicators of uplift may be at least partly due to non-faulting processes, such as Quaternary (intrusive and/or extrusive) volcanic activity associated with evolution of the nearby Lichades volcanic centre.

Keywords: coastal uplift; central Greece; tectonic geomorphology; palaeo-terraces; normal faulting; sea-level

Introduction.

The active normal faulting region of central Greece has been the focus of intense research, due to its relatively high rates of tectonic deformation and the frequent occurrence of damaging moderate magnitude (Ms ≈ 6-7) earthquakes. The structure of central Greece is dominated by a series of roughly WNW-ESE-trending extensional faults. These have created a series of half- (asymmetric) grabens bordered by discontinuous normal faults, the most prominent of which are the Gulf of Corinth and the Evoikos Gulf. Of these two structures, the Evoikos Gulf, and particularly its northern part, is relatively poorly understood in terms of its geodynamic structure and tectonic significance (e.g. Makris et al., 2001). The Arkitsa-Kamena Vourla area occupies the southern part of the northern Evoikos Gulf (Figure 1) and is characterised by a series of very prominent tectonic landforms, notably the large (*ca*. 1000 m elevation) footwall ridge of the Kamena Vourla fault system. This ridge is one of the major geomorphological features of the northern Evoikos Gulf, and is the surface expression of three major left-stepping (normal) fault segments: the Kamena Vourla, the Agios Konstantinos, and the Arkitsa faults (Roberts and Jackson, 1991; Ganas, 1997; Kranis, 1999) (Figure 2 and 3). While it is clear that the northern Evoikos Gulf occupies a zone of accommodation between the two tectonic provinces of the North Aegean Trough (the extension of the North Anatolian fault system) and the Gulf of Corinth (Mitsakaki et al., 2013; see Papanikolaou and Royden, 2007 for regional summary), the interaction between these provinces is not well understood. Recent GPS measurements indicate that the northern Evoikos Gulf is subject to a relatively low magnitude extensional strain field (Hollenstein et al., 2008) which, apparently contradicting the regional geomorphic evidence, should prohibit the development of large faults. Recent research indicates that seismic stress in this area may not necessarily be released with strong earthquakes, but instead with intense microearthquake activity, usually in swarms (Papanastassiou et al., 2001; Papoulia et al., 2006). Indeed, despite the highly prominent nature of the footwall ridge and the presence of very fresh tectonic landforms, the Arkitsa-Kamena Vourla fault system is not known to have hosted any major historical earthquakes (Roberts and Jackson,

1991) and the tectonic (and geomorphic) evolution of the wider Arkitsa-Kamena Vourla area remains poorly constrained.

Goldsworthy and Jackson (2001) argue that the Kamena Vourla fault zone is probably a relatively young system, initiated < 1 Ma ago at the expense of the inland Kalidromon fault (located SW of Mt. Knimis, Figure 1 - see Figure 5a of Goldsworthy and Jackson, 2001). Jackson and McKenzie (1999) identify up to 50 increments of coseismic slip on the Arkitsa fault strand, implying that the Arkitsa segment is the active fault trace in the eastern part of the Kamena Vourla fault zone (Dewez, 2003). More recently however Cundy et al., (2010) have identified and described a prominent raised marginal marine unit (most likely a raised beach) and possibly uplifted beachrock in the coastal zone occupying the hanging wall of the Arkitsa fault, near the archaeological site of Alope, which these authors argue indicates recent uplift (in a series of coseismic events) along a possible active offshore fault strand over the late Holocene. Indeed, offshore geological and geophysical surveys carried out in the northern Evoikos Gulf under the recent AMFITRITI project of the Hellenic Centre for Marine Research (HCMR) (http://amphitriti.ath.hcmr.gr) identify several sites of submarine faulting and seafloor ruptures and the presence of an E–W trending normal fault system offshore of Alope / Arkitsa (Figure 2) is inferred. The activation of this inferred offshore fault offers a mechanism to generate the uplift observed by Cundy et al., (2010) along the Alope coast, although seismic and sub-bottom profiling across the north Evoikos Gulf have (as of yet) failed to discriminate any clear evidence for movement on this offshore fault strand (Sakellariou et al., 2007).

Based on radiocarbon dating of preserved marine fauna and numismatic dating Cundy et al. (2010) propose an average coastal uplift rate at Alope over the last 3000 years in excess of 1 mm/y. While it was unclear to what extent this rapid uplift rate had been sustained over the Late Quaternary, the same authors also note the presence of a series of geomorphological features (terraces (previously noted by Mercier, Dewez and others (Dewez 2003)), cones etc.) between the coast and the Arkitsa fault strand which may indicate longer-term uplift. Here, we present the first detailed multi-proxy study of these geomorphic indicators (via a combined geomorphological, sedimentological

and macro-/micro-fossil approach), focussing in particular on three prominent terraces in the hangingwall of the Arkitsa fault, and evaluate the Late Quaternary evolution and uplift dynamics of this important zone of tectonic strain transfer.

Materials and Methods.

Geomorphological mapping.

Detailed geomorphological mapping at a scale of 1:5000 was performed in a series of field seasons between 2007 and 2010, focusing on the prominent terraces around Arkitsa previously noted by Dewez (2003) and Cundy et al., (2010), and other potential tectonic geomorphic features such as knickpoints, incised alluvial cones or fans, etc. In addition, 1:5000 scale topographic maps were digitised and analysed using GIS technology and terraces and other features visualised and delineated using a digital elevation model (DEM).

Stratigraphy.

Exposed sedimentary sections of terrace material (particularly the "cap-rock" of the terrace surfaces) were cleaned and logged, and intact shell material sampled for ^{14}C dating. The elevations of the exposed units were determined using a Jena 020A theodolite unit, or from 1:5000 scale maps.

Radiometric dating.

Intact carbonate shell material was dated via accelerator mass spectrometry ^{14}C assay (at the Beta Analytic Radiocarbon Dating Laboratory, Florida, U.S.A.). Radiocarbon age calibration (where possible, i.e. on lower elevation, more recent material) was performed using the MARINE04 database (Hughen et al., 2004), via the programme CALIB 5.0 (Stuiver and Reimer, 1993). A ΔR value of - 80 ± 25 years was used, corresponding to the local reservoir age correction for Mediterranean surface waters (Stiros et al., 1992; Pirazzoli et al., 1999).

Microfossil analysis.

Approximately 250 g of material from each terrace was processed for microfossil analysis using a variation of the Glauber's Salt method (Franke, 1922; Wicher, 1942). Indurated sediment samples were soaked in a hot, super-saturated solution of hydrated sodium sulphate and slowly allowed to cool before being frozen overnight. The samples were subsequently defrosted in a microwave oven and the soak-freeze-thaw cycle repeated until the sediments had been sufficiently disaggregated; they were then wet-sieved at >63 μm to remove any finer material. The residue was dried overnight in an oven at 105˚C before being examined under a reflected-light binocular microscope (up to 80 x magnification). Specimens were individually hand-picked from small (~5 g) residue sub-samples and mounted on cavity slides. Identification of the ostracod fauna was made with reference to Meisch (2000).

Results.

Geomorphology: Fluvial systems.

There are four important drainage systems (torrents) in the study area (Figure 3). The longitudinal profiles of the four torrents differ significantly as their evolution depends heavily on the fault tectonism of the area (Figure 4). The Alope and Kounoupitsa torrents are located west of Arkitsa and cross the Arkitsa fault, resulting in convex stream profiles. The Alope torrent flows in a SSW-NNE direction and the Kounoupitsa torrent initially has a W-E direction and then deflects towards the North. Both of these torrents perpendicularly cross the Arkitsa fault zone and exhibit prominent knickpoints. The Alope and Kounoupitsa torrents have both heavily incised into Plio-Pleistocene deposits but the Kounoupitsa torrent exhibits an asymmetric transverse valley cross section with steep cliffs on the south side (Figure 4, inset) due to the tilting of the Arkitsa fault footwall and differential erosion. The Kounoupitsa torrent is further characterized by two distinct cones, the older one being of (presumed) Late Pleistocene age located just north of the Arkitsa fault scarp and the second most recent one of Holocene age located near the shore further north. The older cone is deeply incised up to 26 m at the apex of the fan. The reactivation of the Arkitsa fault seems to be almost continuous until the present day (in accordance with Jackson and

MacKenzie 1999) because the almost 100 m high nickpoint of the Kounoupitsa torrent has not moved upstream from the fault scarp. The other two torrents, the Kynos and Livanates torrents (located south of Arkitsa and flowing to the east), are located wholly on the footwall of the Arkitsa fault, and do not exhibit prominent knickpoints. These two torrents have formed normal alluvial cones which are currently eroding. The Kynos and Livanates torrents depict normal concave longitudinal profiles having evolved mostly on easily-erodible Neogene formations (marls, sandstones and conglomerates).

Geomorphology: Palaeosurfaces and terraces.

In the footwall of the Arkitsa fault four (presumed) Pleistocene-age palaeosurfaces can be identified (Figure 3) which have evolved on Neogene formations composed of conglomerates, sandstones and marls. The oldest of these extends from 400-480 m amsl (above mean sea level), the second 300-390 m, the third 200-280 m, and the most recent one from 140-170 m. The general dip of these palaeosurfaces is towards the south indicating the continuous activity of the Arkitsa fault system.

The geomorphology in the hangingwall of the Arkitsa fault is dominated by a series of deeply-incised colluvial fans and a number of distinct terraces, at elevations of 2-20 m (terrace A), 25-55 m (terrace B) and 50-80 m (terrace C) amsl (Plate 1, Figures 3 and 5). The formation and evolution of the older terrace (C) is contemporaneous with the Kounoupitsa older cone. The higher terraces in the extreme south of this area, around a proposed secondary fault strand at Livanates, are described by Dewez (2003), with the 25-55 m terrace (terrace B) and 50-80 m terrace (terrace C) (Figure 3 and 5) described in the present study correlating with Dewez's T1 and T2 terraces respectively. The terraces are cut into Plio-Pleistocene marls, which are unconformably overlain (most clearly in terraces B and C) by well–cemented arenaceous sediments, forming a prominent "cap–rock". Detailed descriptions of this cap-rock are given below. The two higher and older terraces are deeply dissected down to 27 m by recent fluvial activity. In addition, north of the Arkitsa fault scarp (at 38^{o} 43.680' N; 22^{o}59.340' E) a series of small talus cones have formed during late Pleistocene-Holocene times, which are also deeply incised (Figure 3).

Terrace stratigraphy: Terrace A

This terrace has developed east of the village of Arkitsa and extends for more than 3 km in a NW-SE direction. The terrace has a clear dip to the NE of ~2 %. Its inner edge is found at an elevation of about 20 m. A prominent exposure of terrace A was located at 38^{o} 45.128' N; 23^{o} 01.753' E, at +6 m elevation. While the section was partly-obscured and overgrown, the exposure consisted of 90 cm of highly fossiliferous coarse sandstone unconformably overlying 17 cm of Plio-Pleistocene white silty-clay. The silty-clay unit (in the lower part of the exposure) was relatively unconsolidated, and contained no apparent bedding. The arenacous cap-rock in the upper part of the exposure consisted of a coarse, well-rounded and sorted sand with grit and occasional small (<1 cm) sub-rounded limestone pebbles. Macrofossil remains were common and included both intact and disaggregated bivalve and gastropod shell material, with identifiable fragments (*ca*. 5mm in size) consisting entirely of juvenile *Mytilus* sp. (possibly *Mytilus galloprovincialis*). Shell remains were distributed highly heterogeneously; in some parts they were almost absent, whereas in other areas they comprised 30–50 % of the cap-rock. Occasional disarticulated juvenile ostracod remains of *Cyprideis torosa* were present, as well as rare single valves of juvenile *Candona* sp.

Terrace stratigraphy: Terrace B

This terrace is the most prominent in the area, and extends for 7.5 km in an E-W direction. Its elevation increases towards the east, so the inner edge rises from a height of 25 m in the west to 55m in the east. The terrace is tilted towards the south with a dip of 1 %. A clear roadside exposure of terrace B was found at 38^{o} 44.517' N; 23^{o} 01.823' E, at +30 m elevation. The exposure consisted of a 1 m-thick unit of well-cemented sandstone, unconformably overlying a lower unit (1.6 m thick) of thinly-bedded marly silts and sands. Bed thickness in this thinly-bedded lower (Plio-Pleistocene) unit was 1 – 5 cm, dipping at 16^{o} WNW. The upper sandstone (cap-rock) unit consisted of a well-cemented medium sand and silt, with sub-rounded to rounded grits and pebbles of limestone and chert composition. Pebbles ranged between 1 and 3 cm in diameter. Small (< 1 cm) isolated gastropod fragments (apparently *Viviparus* sp.)

were locally present. A more complete and extensive sequence of the well-cemented arenaceous cap-rock was found in a roadside cut and adjacent private land at 38° 44.589' N; 23° 02.002' E, showing 1.8 m of exposure, consisting of 0.55 m of well-cemented sandstone (stratigraphy as detailed above) overlying 1.25 m of bedded *Viviparus* sp.-rich well-cemented medium to coarse sand, with sub-angular to sub-rounded chert (and occasional limestone) pebbles, up to 3 cm diameter. Intact *Viviparus* sp. shells occurred throughout this unit, locally concentrated into coquina-type beds. Juvenile valves of the ostracods *Cyprideis torosa* and *Candona* spp. were common throughout, valves of *Ilyocpris* sp. and *Tyrrhenocythere* sp. (also juvenile) were also present but were considerably rarer.

Terrace stratigraphy: Terrace C

This terrace extends for 5 km in an E-W direction. Its elevation increases towards the east, so the inner edge from a height of 50 m in the west reaches 80 m in the east. The terrace is tilted towards the south having a dip of 1.5 %. A prominent exposure in a road cut (adjacent to the main access road to Arkitsa port) at 38° 44.622' N; 23° 01.567' E, +50 m elevation, showed *ca*. 0.5–0.7 m of well-cemented, gastropod-rich, sandstone unconformably overlying yellow-white marls. The stratigraphy of the lower (Plio-Pleistocene) marls is described in detail in Dewez (2003). The upper sandstone (cap-rock) unit was rich in intact and fragmented *Viviparus* sp. (Dewez's "*Viviparus* cayrock") and other gastropods (including rare *Valvata piscinalis*), sometimes forming coquina-type lenses, in a medium to coarse sand matrix. Ostracod remains were rare, however, and limited to occasional juvenile, disarticulated valves of *Cyprideis torosa* and *Candona* spp.. The sand contained sub-rounded to rounded limestone and chert grit clasts, and rounded to sub-rounded limestone, chert and (sporadic) mafic pebbles, of 4–5 cm diameter. The structure of the cap-rock layer here was relatively complex, as the *ca*. 100 m of horizontal exposure indicated the presence of two unconformable cap-rock layers (Plate 2), an upper (horizontally-bedded) unit above a lower (slightly older) cap-rock unit with bedding dipping at 5° E. At a small quarry N of this road cut (38° 44.642' N; 23° 01.528' E), where the cap-rock has been removed for use locally as a building stone, intact *Viviparus* sp. fragments were less frequent, although the section contained a series of highly abraded broken shell or coquina layers.

256

257 **Radiocarbon dating**

258 Two valves of *Mytilus galloprovincialis* collected from terrace A (at +6 m) gave
259 conventional radiocarbon ages of 36200 ± 340 BP and 40530 ± 500 BP (Table 1). An
260 intact *Viviparus* sp. specimen from terrace B (at +30 m) gave a further conventional
261 radiocarbon age of >43500 BP (Table 1).

262

263 **Discussion**

264 The main factor controlling the late Quaternary deposits of the Northern Evoikos Gulf
265 coast and sea floor was global sea level change caused by the numerous glacial-
266 interglacial cycles of the Pleistocene. Exchange of water masses with the Aegean Sea is
267 restricted via (a) the narrow and shallow Oreos-Trikeri straits, which have a maximum
268 depth of approximately 45 m and a mean width of 4 km, and (b) the artificially
269 maintained Euripus Channel (length 60 m, width 40 m, depth 8.5 m) in the southeast
270 of the region (Figure 1). The maximum pre-Holocene sill depth in the Oreos-Trikeri
271 straits is currently approximately 45 m below sea-level (bsl), although Van Andel and
272 Perissoratis (2006) argue for a late glacial sill depth at about 55 m bsl based on high-
273 resolution seismic profiling data. The Northern Evoikos Gulf was isolated from the
274 Aegean Sea at *ca*. 50,000 yrs BP (Figure 6) and became a lake during Oxygen Isotope
275 Stage (OIS) 3 and 2. The lake began to fill with seawater as soon as sea level reached
276 the critical sill depth at the Oreos-Trikeri straits at about 10,500 ^{14}C BP (Lambeck,
277 1996).

278

279 Of the terraces described here, only the lowest (terrace A) is datable via ^{14}C (Table 1);
280 the higher terrace B gives a date which exceeds the dating range of ^{14}C (> 43,500 BP).
281 While further dating using U-series methods may better constrain the ages of the
282 upper terraces B and C, given the thin, delicate nature of the preserved *Viviparus*
283 fossils, and the high likelihood that these gastropods may act as open systems in terms
284 of U-exchange, such dating is unlikely to definitively ascribe an accurate age to the
285 upper cap rocks. The ^{14}C dates from terrace A (*ca*. 36,000 – 41,000 BP) specify its
286 formation at a period of low regional and global sea-level, on the margins of the

Evoikos glacial lake. While water levels in the glacial lake clearly fluctuated due to climatic variations, the dates for terrace A correlate with OIS-3, a period with warmer and wetter intervals, which Van Andel and Perissoratis (2006) tentatively correlate with a cluster of erosional submarine terraces incised in the Evoikos Gulf floor between 50 and 70 m bsl. The sedimentology of the terrace A cap-rock (i.e. coarse, well-rounded and sorted sand with grit and occasional small [<1 cm] sub-rounded limestone pebbles) indicates deposition in the higher-energy lake shallow margins, although the dominant faunal remains, those of juvenile *Mytilus* sp. (possibly *Mytilus galloprovincialis*), indicate deposition in at least a brackish environment (e.g. Ceccherelli and Rossi 1984). The age of this terrace correlates with a period of relative high stand, when sea-levels were close to the sill depth (Shackleton 1987, Labeyrie et al 1987 and discussion in Van Andel and Perissoratis 2006), which may explain the dominance of *Mytilus* sp.. This interpretation is further supported by the microfossil assemblage. *Cyprideis torosa* are euryhaline ostracods, tolerating a broad range of salinities from almost freshwater to hypersaline (but they are never fully marine) (Meisch, 2000). They tend to occupy estuaries, lagoons, brackish-water bays and shallow near-shore littoral environments that have sandy/muddy substrates with some algal/organic cover. Their valves are moderately robust and so they can tolerate moving water and moderate energy conditions, further evidenced here by a lack of larger instars. On the other hand, candoniid ostracods are not usually associated either with elevated salinities or high-energy environments (Meisch, 2000), suggesting that the rare *Candona* sp. valves here may have been washed in from the local catchments.

Regardless of the precise (palaeo) lake level, the current elevation of terrace A compared to the estimated late glacial Oreos-Trikeri sill depth of 55 m bsl indicates considerable uplift over the last *ca*. 40,000 years. Based on the age of the *Mytilus* sp. at +6 m and a sill depth of 55 m bsl, a minimum average uplift rate of 1.5 mm/y can be derived (i.e. 61 m in 40,000 years, which is a minimum estimate due to uncertainties in palaeo-lake level). Considering the higher terraces, while the ages of terraces B and C are not well-constrained (> 43,500 BP), their sedimentological characteristics (arenaceous to conglomeratic) and fossil content indicates their formation in a

318 freshwater lake margin. *Viviparus* sp. prefer shallow freshwater or (occasionally)
319 oligosaline habitats with muddy substrates such as might be found on the margins of
320 slow-moving lowland rivers and the littoral areas of large lakes (e.g. Glöer, 2002).
321 Coupled with the presence of freshwater (*Candona* spp., *Ilyocypris* sp.) and oligosaline
322 (*Cyprideis torosa*, *Tyrrhenocythere* sp.) ostracods (e.g. Meisch, 2000; Griffiths, 2002;
323 Alvarez-Zarikian, 2008), the faunal evidence points to a shallow, freshwater or very
324 slightly brackish lake / lagoonal margin. Based on the discussion above, it is likely that
325 these terraces were formed in earlier phases of OIS 3 and OIS 4 during relative high
326 stand periods, and then uplifted to their present elevations. Indeed, Van Andel and
327 Perissoratis (2006) note a series of submerged erosional terraces in the northern
328 Evoikos Gulf clustered around discrete depth intervals, and probably correlating with
329 lake level fluctuations over OIS 2-4. Sea-level curves (Figure 6) suggest that terrace B
330 may have been formed around 55,000–60,000 yrs BP and terrace C prior to about
331 70,000 yrs BP. Further support for this inference comes from the terrestrial pollen
332 record, including evidence from the well-dated lacustrine sequences from Ioannina in
333 the north-west of Greece (Tzedakis et al., 2002) and Kopais on the Boetian plain,
334 located less than 40 km south of Arkitsa (Tzedakis, 1999). Palynological data from both
335 of these sites indicate the presence of intermediate forest (including a temperate tree
336 component) for part of the Middle Pleniglacial between *ca*. 50,000 and 59,000 yrs BP
337 (encompassing the proposed formation of terrace B), and fully-forested interstadial
338 conditions between *ca*. 68,000 and 83,000 yrs BP (encompassing the proposed
339 formation of terrace C). During these relatively wet and warm periods, sea-level was at
340 a depth of *ca*. 60 m below present sea level or higher, below but not far from the
341 proposed sill depth of 55 m. If correct these estimates would suggest that terrace B
342 was uplifted by *ca*. 85 m (i.e. 60 m + 25 m [lowest position of the inner terrace edge]),
343 and terrace C by *ca*. 110 m (i.e. 60 m +50m [lowest position of the inner terrace edge]),
344 having uplift rates of about 1.4 mm/y (85 m/60,000 yrs for terrace B and 110 m/75,000
345 yrs for terrace C).

346 Terrace data therefore suggest uplift at average rates of 1–1.5 mm/y beyond the
347 Holocene in the late Pleistocene, to at least 40,000 yrs BP. This estimated uplift rate is
348 significantly higher than the long-term (footwall) uplift rate of 0.2 mm/y calculated by

Goldsworthy and Jackson (2001) for the eastern end of the Arkitsa fault segment (also reported by Walker et al., (2010)), and while it agrees well with Late Holocene uplift rates of 1–1.4 mm/y proposed by Cundy et al., (2010) based on nearby slightly uplifted marginal marine units around Alope, it poses significant problems in terms of fault dynamics and extension rates in the area. While rupture of the offshore fault inferred by Sakellariou et al., (2007) and Cundy et al., (2010) provides a mechanism for recent coseismic coastal uplift in the Alope area, sustained coastal uplift on this fault of 1 – 1.5mm/y requires anomalously high slip and extension rates. Specifically, if a footwall-hangingwall partition of 1:2 is adopted (following McNeill et al.'s (2005) range of 1:1.2 to 1:2.2 derived from active faults in the Gulf of Corinth rift, which have similar dip to those in the Arkitsa area), then the resultant slip rate on this offshore fault would be *ca*. 4 – 6 mm/y, with an extension rate of 3 – 4.5 mm/y. This slip rate is much higher than recent estimates using continuous GPS stations in central Greece (Chousianitis et al., 2013), which (a) indicate that most of the extensional strain across the northern Evoikos Gulf is accommodated by the Arkitsa fault, and (b) suggest at most a 1.2 - 1.5mm/y slip rate on other active faults in this area. The high uplift rate estimates are similarly problematic given that renewed activity on the onshore Arkitsa fault will down-throw the terraces, and require even higher slip rates on offshore fault systems. In this respect, of note is the apparent presence in terrace C of two unconformable cap-rock layers (Plate 2) with differing bedding dip angles. The contrast in dip angle is laterally extensive and, although the section is partly obscured by vegetation, the unconformable relationship between the two units is clear (Plate 2). This indicates formation of the cap-rock here in at least two phases, interrupted by an episode of slight tilting and erosion, possibly related to local coseismic movement from the activity of the Arkitsa fault. In other words, after the formation of the lower cap-rock, it is possible that the Arkitsa fault reactivated and caused the tilting of this formation towards the fault. The proximity of this site (some tens of metres) to the scarp of the Arkitsa fault and its position on the fault's hanging wall supports this hypothesis. Subsequently, the newer cap-rock was formed in discordance with the former one. This event should have happened during the formation of terrace C, i.e. possibly around 70,000–75,000 yrs BP. The existence of a fresh strip of fault scarp at the base of the Arkitsa fault, attributed to Holocene activity (Jackson and MacKenzie 1999), and

the geomorphology of the fluvial systems which cross the fault, indicates that the Arkitsa fault remains active.

Given the excessively high, long-term offshore fault slip rates required to generate purely extensional fault-driven uplift of the terraces to their present elevation, some other explanation must therefore be found for their presence at up to 80m above current sea-level. Possible causes are non-extensional local uplift, or formation of the terraces at elevations above the contemporary shoreline due to local damming of the Evoikos glacial lake. Two volcanic centres are present (the Lichades and Chronia volcanic centres) to the northwest and northeast of the Arkitsa area which were activated during the Pliocene and Quaternary (Pe-Piper and Piper 1989, 2002; Lambrakis and Kalergis, 2005, although the Chronia volcanic centre is of questionable, possibly older, age, [Karasththeis et al., 2011]), and a magma chamber at 8km depth has been detected north of Arkitsa (Karasththeis et al., 2011) which is argued to be the source of the widespread hydrothermal activity observed in the northern part of the Evoikos Gulf. Basaltic sill intrusion could potentially generate local uplift, and extrusion of lava cause local shoreline changes, particularly near to the Oreos-Trikeri straits, and "barriering" or damming of lakes at higher elevations. The exact causal mechanism of terrace development and uplift remains enigmatic, and further detailed studies of these volcanic centres and their influence on palaeo-shoreline geomorphology and local uplift (coupled with offshore geophysical work in the NW Evoikos Gulf to better constrain offshore fault slip and activity and the relationship between onshore and offshore (submerged) terraces) are needed to better constrain the Late Quaternary uplift pattern in this area, and determine the relative roles of extensional faulting and other regional processes (e.g. volcanic centre activity) in driving palaeoterrace formation and uplift.

Conclusions

A combined geomorphological, sedimentological and macro-/micro-fossil approach has been used to evaluate the Late Quaternary tectonic evolution and uplift of the Arkitsa area, in the eastern part of the Arkitsa-Kamena Vourla fault system, focusing on prominent terraces present in the hangingwall of the Arkitsa fault. Three distinct raised

glacio-lacustrine terraces, and previously reported uplifted marginal marine deposits, indicate sustained uplift of the coastline at a rate of 1 – 1.5 mm/y over at least the last 40,000 years, possibly to 75,000 BP. While movement on an offshore normal fault strand may partly explain this (and more recent) coastal uplift, purely fault-driven uplift requires anomalously high fault slip and extension rates over the Late Quaternary. Consequently, the development of the terraces and other geomorphic indicators of uplift may be at least partly due to non-extensional faulting mechanisms, such as Quaternary (intrusive and/or extrusive) volcanic activity associated with evolution of nearby volcanic centres. Further detailed studies of these volcanic centres and their influence on palaeo-shoreline geomorphology and local uplift, coupled with offshore geophysical work in the NW Evoikos Gulf to better constrain offshore fault slip and activity, are needed to determine the relative roles of extensional faulting and other processes in driving palaeo-terrace formation and uplift around Arkitsa.

Acknowledgements.

Tim Cane (University of Sussex) is thanked for laboratory assistance. We are also indebted to Professor James Jackson and a further (anonymous) reviewer who provided in-depth comments which significantly improved the overall quality of this paper.

References cited.

Alvarez-Zarikian, C.A., Soter, S., Katsonopoulou, D., 2008. Recurrent submergence and uplift in the area of Ancient Helike, Gulf of Corinth, Greece: microfaunal and archaeological evidence. Journal of Coastal Research, 24 (1A), 110-125.

Armijo, R., Lyon-Caen, H., Papanastassiou, D., 1992. East-west extension and Holocene normal fault scarps in the Hellenic arc. Geology, 20, 491-494.

Ceccherelli, V. U., Rossi R., 1984. Settlement, growth and production of the mussel Mytilus galloprovincialis. Marine Ecology Progress Series, 16, 173-184.

441 Chousianitis, K., Ganas, A., Gianniou, M., 2013. Kinematic interpretation of present-day
442 crustal deformation in central Greece from continuous GPS measurements.
443 Journal of Geodynamics, 71, 1– 13. doi:10.1016/j.jog.2013.06.004

444 Cundy A.B., Gaki-Papanastassiou K., Papanastassiou D., Maroukian H., Frogley M.R.,
445 Cane T., 2010. Geological and geomorphological evidence of recent coastal uplift
446 along a major Hellenic normal fault system (the Kamena Vourla fault zone, NW
447 Evoikos Gulf, Greece). Marine Geology, 271, 156-164.

448 Dewez, T.J.B., 2003. Geomorphic markers and digital elevation models as tools for
449 tectonic geomorphology in Central Greece. Unpublished PhD thesis, Brunel
450 University, Uxbridge, U.K., 173 pp.

451 Franke, A., 1922. Die Präparation von Foraminiferen und anderen mikroskopischen
452 Tierresten, p. 509-533. In Keilhack, K. (ed.), Lehrbuch der praktischen Geologie,
453 Mineralogie, und Palaeontologie (fourth edition). Enke-Verlag, Stuttgart.

454 Ganas, A., 1997. Fault segmentation and seismic hazard assessment in the Gulf of Evia
455 rift, Central Greece. Unpublished PhD Thesis, University of Reading, Reading, U.K.
456 368 pp.

457 Glöer, P., 2002. Süßwassermollusken Nord und Mitteleuropas. Bestimmungsschlüssel,
458 Lebensweise, Verbreitung. ConchBooks, Hackenheim., 327 pp.

459 Goldsworthy, M., Jackson, J., 2001. Migration of activity within normal fault systems:
460 examples from the Quaternary of mainland Greece. Journal Structural Geology,
461 23, 489-506.

462 Griffiths, S.J., Griffiths, H.I., Altinsacli, S., Tzedakis, P.C., 2002. Interpreting the
463 Tyrrhenocythere (Ostracoda) signal from Palaeolake Kopais, central Greece.
464 Boreas, 31, 250-259.

465 Hollenstein Ch., Muller, M.D., Geiger, A., Kahle, H.-G., 2008. Crustal motion and
466 deformation of Greece from a decade of GPS measurements, 1993 – 2003.
467 Tectonophysics, 449, 17-40.

468 Hughen, K.A., Baillie, M.G.L., Bard, E., Bayliss, A., Beck, J.W., Bertrand, C.J.H., Blackwell,
469 P.G., Buck, C.E., Burr, G.S., Cutler, K.B., Damon, P.E., Edwards, R.L., Fairbanks,
470 R.G., Friedrich, M., Guilderson, T.P., Kromer, B., McCormac, F.G., Manning, S.W.,
471 Bronk Ramsey, C., Reimer, P.J., Reimer, R.W., Remmele, S., Southon, J.R., Stuiver,
472 M., Talamo, S., Taylor, F.W., van der Plicht, J., Weyhenmeyer, C.E., 2004.
473 Marine04 Marine radiocarbon age calibration, 26 - 0 ka BP, Radiocarbon, 46,
474 1059-1086.

475 Jackson, J., Mackenzie, D., 1999. A hectare of fresh striations on the Arkitsa Fault,
476 central Greece. Journal Structural Geology, 21, 1-6.

477 Karastathis, V.K., Papoulia, J., Di Fiore, B., Makris, J., Tsambas, A.,Stampolidis A.,
478 Papadopoulos, G.A., 2011. Deep structure investigations of the geothermal field
479 of the North Euboean Gulf,Greece, using 3-D local earthquake tomography and
480 Curie Point Depth analysis. Journal of Volcanology and Geothermal Research,
481 206, 106–120. doi:10.1016/j.jvolgeores.2011.06.008.

482 Kranis, H.D., 1999. Fault zone neotectonic activity in Lokris. Unpublished PhD Thesis.
483 Dept. of Geology, Athens University, Greece.

484 Labeyrie, L.D., Duplessy, J.C., Blanc, P.L., 1987. Variations in the mode of formation and
485 temperature of oceanic deep waters over the past 125,000 years. Nature 327,
486 477–482.

487 Lambeck, K., 1996. Sea-level change and shore-line evolution: a general framework of
488 modelling and its application to Aegean Greece since Palaeolithic time. Antiquity
489 70, 588–611.

490 Makris, J., Papoulia, J., Papanikolaou, D., Stavrakakis, G. 2001. Thinned continental
491 crust below northern Evoikos Gulf, central Greece, detected from deep seismic
492 soundings. Tectonophysics, 341, 225-236.

493 McNeill, L.C., Cotterill, C.J., Henstock, T.J., Bull, J.M., Stefatos, A., Collier, R.,
494 Papatheoderou, G., Ferentinos G., Hicks, S.E., 2005. Active faulting within the
495 offshore western Gulf of Corinth, Greece: Implications for models of continental
496 rift deformation. Geology, 33/4, 241–244. doi: 10.1130/G21127.1

497 Meisch, C., 2000. Freshwater Ostracoda of Western and Central Europe. In:
498 Schwoerbel, J., Zwick, P. (eds.), Süsswasserfauna von Mitteleuropa 8/3.
499 Spektrum Akademischer Verlag, Heidelberg, 522pp.

500 Mitsakaki, C., Sakellariou, M.G., Tsinas, D., 2013. A study of the crust stress field for the
501 Aegean region (Greece). Tectonophysics, 597–598, 50–72.
502 doi:10.1016/j.tecto.2012.10.003.

503 Papanastassiou, D., Stavrakakis, G., Makaris, D., 2001. Recent micro-earthquake
504 activity at northern Evoikos gulf, central Greece. Bulletin of the Geological
505 Society of Greece, XXXIV, 1567-1572.

506 Papanikolaou, D.J., Royden, L.H., 2007. Disruption of the Hellenic arc: late Miocene
507 extensional detachment faults and steep Pliocene-Quaternary normal faults - or
508 what happened at Corinth? Tectonics, 26, TC5003 doi:10.1029/2006TC002007.

509 Papoulia, J., Makris, J., Drakopoulou, V., 2006. Local seismic array observations at
510 north Evoikos, central Greece, delineate crustal deformation between the North
511 Aegean Trough and Corinthiakos Rift. Tectonophysics, 423, 97-106.

512 Pe-Piper, G., Piper, J.W., 1989. Spatial and temporal variation in Late Cenozoic back-arc
513 volcanic rocks, Aegean Sea Region. Tectonophysics, 169, 113–134.

514 Pe-Piper, G., Piper, D.J.W., 2002. The igneous rocks of Greece, the anatomy of an
515 orogen. Beitrage regionalen geologie der erde. Gebruder borntraeger. 573 pp.

516 Pirazzoli, P.A., Stiros, S.C., Arnold, M., Laborel, J., Laborel-Deguen, F., 1999. Late
517 Holocene coseismic vertical displacements and tsunami deposits near Kynos,
518 Gulf of Euboea, central Greece. Physics and Chemistry of the Earth (A), 24, 361-
519 367.

520 Roberts, S., Jackson, J., 1991. Active normal faulting in central Greece: an overview, in:
521 Roberts, A.M., Yielding, G., Freeman, B. (Eds), The Geometry of Normal Faults,
522 Geological Society Special Publications 56, Geological Society, London, pp. 125 -
523 142.

524 Sakellariou, D., Rousakis, G., Kaberi, H., Kapsimalis, V., Georgiou, P., Kanellopoulos, Th.,
525 Lykousis, V., 2007. Tectono-sedimentary structure and Late Quaternary evolution
526 of the North Evia Gulf basin, central Greece: preliminary results. Bulletin of the
527 Geological Society of Greece, XXXX, 451–462.

528 Shackleton, N.J., 1987. Oxygen isotopes, ice volume and sea level. Quaternary Science
529 Reviews, 6, 183–190.

530 Stiros, S.C., Arnold, M., Pirazzoli, P.A., Laborel, J., Laborel, F., Papageorgiou, S., 1992.
531 Historical coseismic uplift on Euboea Island, Greece. Earth and Planetary Science
532 Letters, 108, 109-117.

533 Stuiver, M., Reimer, P.J., 1993. Extended 14C database and revised CALIB radiocarbon
534 calibration program. Radiocarbon, 35, 215-230

535 Tzedakis, P.C., 1999. The last climatic cycle at Kopais, central Greece. Journal of the
536 Geological Society of London, 156, 425-434.

537 Tzedakis, P.C., Lawson, I.T., Frogley, M.R., Hewitt, G.M.. Preece, R.C., 2002. Buffered
538 tree population changes in a Quaternary refugium: evolutionary implications.
539 Science 297, 2044-2047.

540 van Andel, T.H., Perissoratis, C., 2006. Late Quaternary depositional history of the
541 North Evoikos Gulf, Aegean Sea, Greece. Marine Geology, 232, 157-172.

542 Walker, R.T., Claisse, S., Telfer, M., Nissen, E., England, P., Bryant, C., Bailey, R., 2010.
543 Preliminary estimate of Holocene slip rate on active normal faults bounding the
544 southern coast of the Gulf of Evia, central Greece. Geosphere, 6/5; 583–593; doi:
545 10.1130/GES00542.1

546 Waelbroeck, C., Labeyrie, L., Michel, E., Duplessy, J.C., McManus, J.F., Lambeck, K.,
547 Balbon, E., Labracherie, M., 2002. Sea-level and deep water temperature
548 changes derived from benthic foraminifera isotopic records. Quaternary Science
549 Reviews, 21, 295–305

550 Wicher, C.A., 1942. Praktikum der angewandten Mikropaläontologie. Gebrüder
551 Borntraeger, Berlin-Zehlendorf, 143 pp.

552

553

554
555 **Figures and Tables:**
556
557 Table 1: Radiocarbon and numismatic dates from the Arkitsa terraces and uplifted
558 marginal marine units exposed around Alope.
559
560 Figure 1. Location of the Northern Evoikos gulf in central Greece. Relief shading shows
561 the general bathymetry of the Gulf and the topography of the coast and inland
562 areas. The location of the Oreos-Trikeri straits in the north and Euripus channel
563 in the south, and location and names of major fault systems (K.V.: Kamena
564 Vourla, A.G.: Agios Konstantinos, Ar: Arkitsa, At.: Atalanti, T: Tragana, M:
565 Malesina, Efv.: Evia fault zone) are also marked. Stars indicate the Lichades (L)
566 and Chronia (C) volcanic centers. Projection/datum used: Hellenic Geodetic
567 Reference System 1987 - non-geocentric datum.
568 Figure 2. Geological setting and tectonic structure of the Arkitsa-Kamena Vourla area,
569 north Evoikos Gulf, central Greece. After Institute of Geology and Mineral
570 Exploration (IGME) sheets (1:50,000 scale): Elateia (1967), Pelasgia (1957),
571 Livanatai (1965) and Istiaia (1984).
572 Figure 3. Geomorphological map of study area: Kynos-Arkitsa-Alope coastal zone.
573 Topographic data taken from 1:5000 scale topographic maps (Hellenic Military
574 Geographical Service, 1979). Line CS_1 shows location of cross-section for Figure 4
575 inset.
576 Figure 4. The longitudinal profiles of the Alope, Kounoupitsa, Kynos and Livanates
577 torrents. Inset gives the N-S cross section of the Kounoupitsa torrent, marked as
578 line CS_1 in Figure 3.
579 Figure 5: Digital elevation model (20m x 20m) of the Arkitsa area, highlighting terrace A
580 (green), B (orange) and C (blue). Vertical exaggeration is x5. Google Earth
581 imagery reference: Google earth V 7.1.2.2041. (10/7/2013). Arkitsa, Greece.
582 38°44.041' N; 22°59.735' E; Eye alt. 1500m. Digital Globe 2014.
583 http://www.earth.google.com [January 15, 2014].

584 Figure 6. Global eustatic sea-level curves for the last *ca*. 80 kyr after Shackleton (1987)
585 and Waelbroeck et al., (2002), illustrating major global sea-level trends during
586 the Late Quaternary. OIS 3 and OIS 4 are labeled, and the estimated depth of the
587 Oreos-Trikeri sill during late glacial periods is also marked (after Van Andel and
588 Perissoratis 2006).

589

590 Plate 1: Panoramic view of the 3 prominent terraces in the area of Arkitsa (view east,
591 from 38°44.50' N; 23°00.50' E). From left to right: terrace A (2-20 m), terrace B
592 (25-55 m), terrace C (50-80 m).

593 Plate 2: Panorama of terrace C exposure (view towards east, from 38° 44.622' N; 23°
594 01.567' E), showing two unconformable layers of cap-rock. Note contrast in dip
595 angle (see text for further discussion). Figure for scale is 1.8m in height.

596

597

Sample[1]	Species / type	Sample elevation (above HWL)	Conventional ^{14}C age (a BP, ± 1 σ)	Lab. number	$^{13}C/^{12}C$ ($^{o}/_{oo}$)	Calibrated age (a BP)[2]	Source
Shell	*Viviparus* sp.	30m	>43500 BP	Beta-285990	-7.0	-	This study
Shell	*Mytilus* sp. *(prob. M.galloprovincialis)*	6m	40530 ± 500 BP	Beta-258442	+0.6	-	This study
Shell	*Mytilus* sp. *(prob. M.galloprovincialis)*	6m	36200 ± 340 BP	Beta-285989	-0.5	-	This study
Shell	*Cerithium* sp.	1.1 – 1.6 m	2900 ± 40 BP	Beta-218939	+0.8	916 – 724 BC	Cundy et al. (2010)
Shell	*Cerithium* sp.	1.1 – 1.6 m	2980 ± 40 BP	Beta-218940	+0.7	1001 – 783 BC	Cundy et al. (2010)
Shell	*Spondylus* sp.	0.9 – 1.5 m	3430 ± 40 BP	Beta-236948	+1.6	1581 – 1332 BC	Cundy et al. (2010)
Coin	Base metal Roman *nummus*	1.1 – 1.6 m	–	–	–	AD 378 – 383[3]	Cundy et al. (2010)
Shell	Gastropod (sp. indet.)	0.30 m	1820 ± 40 BP	Beta-236949	-0.1	AD 394 - 623	Cundy et al. (2010)

[1] Shell samples pretreated by etching with HCl.
[2] Calibration performed using the MARINE04 database (Hughen et al 2004), using the programme CALIB 5.0 (Stuiver and Reimer, 1993). A delta R value of -80 ± 25 years was used, corresponding to the local age reservoir of Mediterranean surface waters (Stiros et al 1992, Pirazzoli et al 1999). Values presented show a 2σ error margin.
[3] Age based on identification of coin as *Reparatio Reipub* type. Richard Abdy, Curator, Roman Coins, British Museum, pers. comm. See Cundy et al. (2010) for discussion.

Table 1

Figure 1

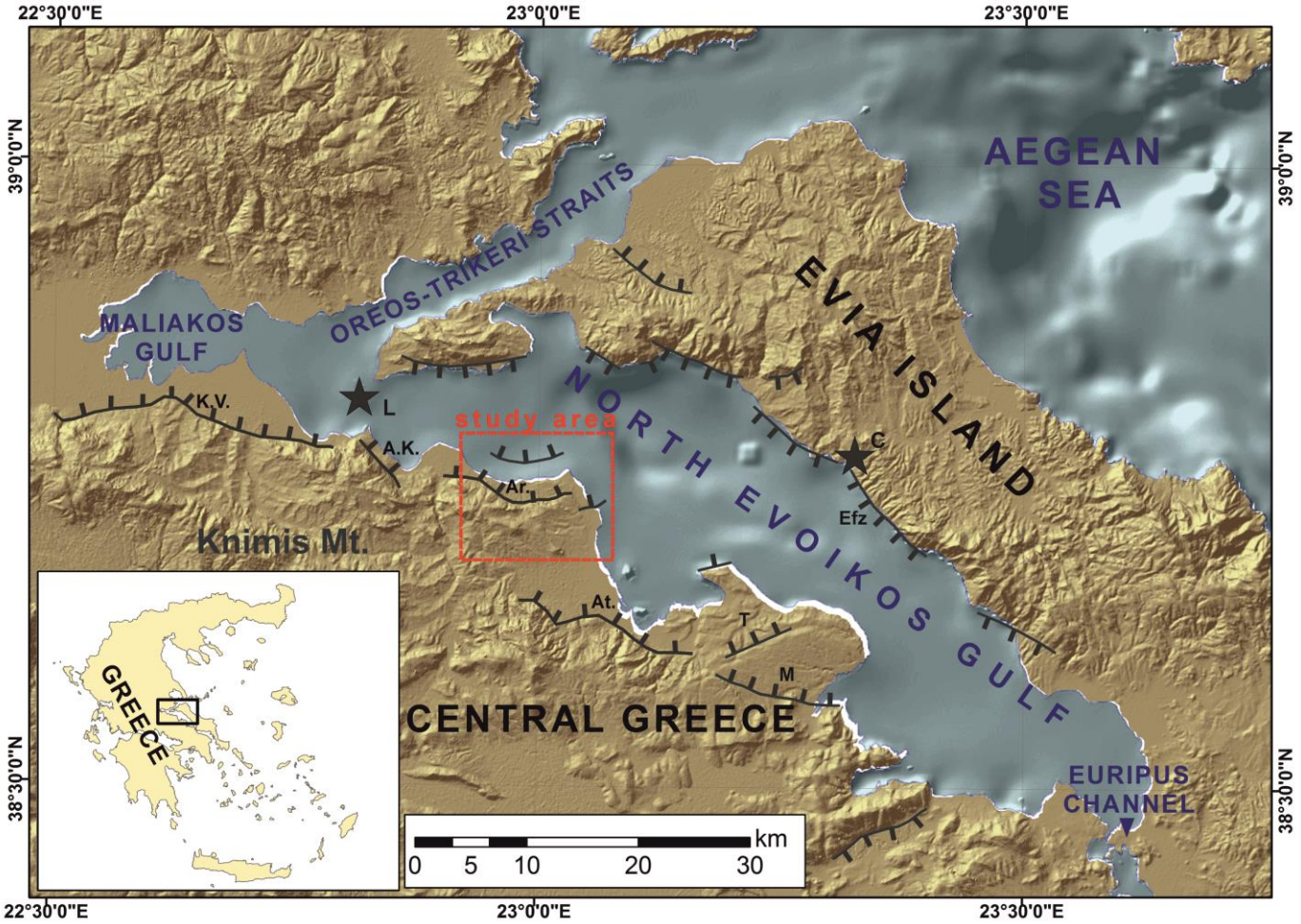
22°30'0"E
23°0'0"E
23°30'0"E
39°0'0"N
38°30'0"N
AEGEAN SEA
OREOS-TRIKERI STRAITS
MALIAKOS GULF
EVIA ISLAND
NORTH EVOIKOS GULF
K.V.
L
A.K.
study area
Ar.
C
Efz
Knimis Mt.
At.
T
M
CENTRAL GREECE
EURIPUS CHANNEL
GREECE
km
0 5 10 20 30

Figure 2

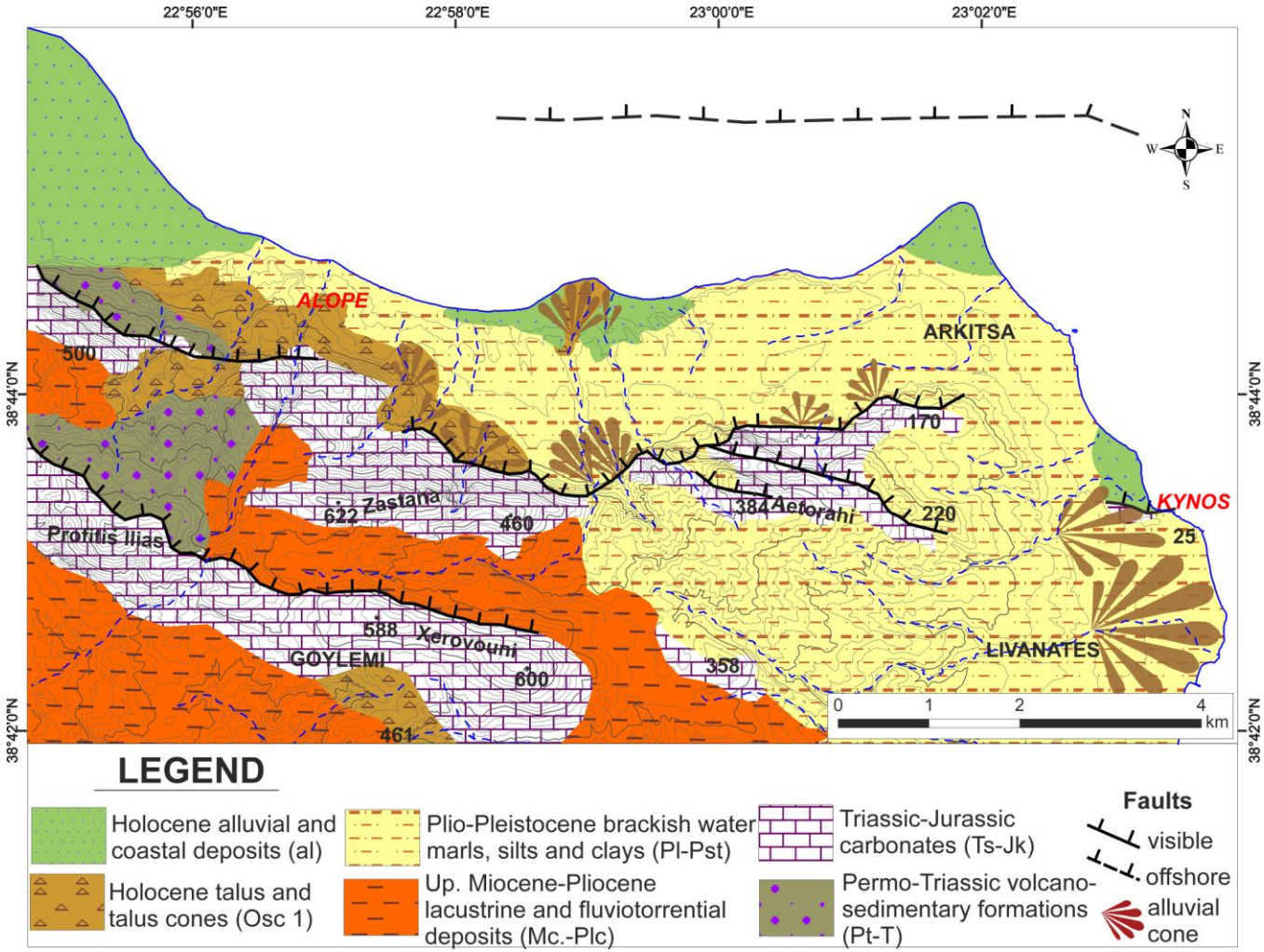
22°56'0"E
22°58'0"E
23°00'0"E
23°02'0"E
38°44'0"N
38°42'0"N
N
W
E
S
ALOPE
ARKITSA
KYNOS
LIVANATES
GOYLEMI
500
622
Zastana
460
Profitis Ilias
588
Xerovouni
600
461
384
Aetorahi
170
220
358
25
0
1
2
4
km
LEGEND
Holocene alluvial and coastal deposits (al)
Holocene talus and talus cones (Osc 1)
Plio-Pleistocene brackish water marls, silts and clays (Pl-Pst)
Up. Miocene-Pliocene lacustrine and fluviotorrential deposits (Mc.-Plc)
Triassic-Jurassic carbonates (Ts-Jk)
Permo-Triassic volcano-sedimentary formations (Pt-T)
Faults
visible
offshore
alluvial cone

Figure 3

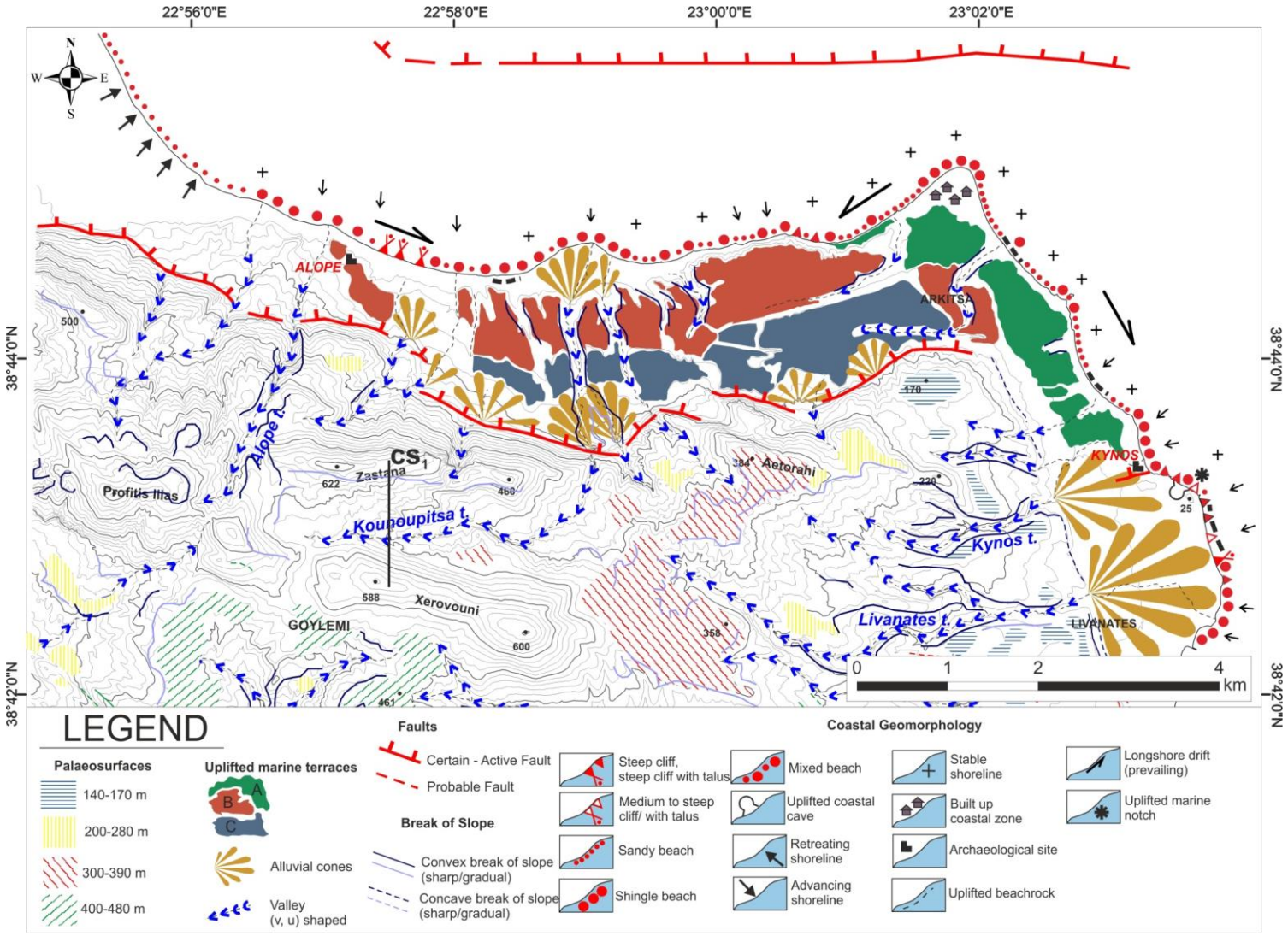
22°56'0"E
22°58'0"E
23°00'0"E
23°02'0"E
38°44'0"N
38°42'0"N
N
W
E
S
ALOPE
ARKITSA
KYNOS
LIVANATES
Alope t.
Koumoupitsa t.
Kynos t.
Livanates t.
Profitis Ilias
Zastana
Xerovouni
GOYLEMI
Aetorahi
CS1
500
622
460
588
600
461
384
470
220
25
358
0 1 2 4
km
LEGEND
Palaeosurfaces
140-170 m
200-280 m
300-390 m
400-480 m
Uplifted marine terraces
A
B
C
Alluvial cones
Valley
(v, u) shaped
Faults
Certain - Active Fault
Probable Fault
Break of Slope
Convex break of slope
(sharp/gradual)
Concave break of slope
(sharp/gradual)
Coastal Geomorphology
Steep cliff,
steep cliff with talus
Medium to steep
cliff/ with talus
Sandy beach
Shingle beach
Mixed beach
Uplifted coastal
cave
Retreating
shoreline
Advancing
shoreline
Stable
shoreline
Built up
coastal zone
Archaeological site
Uplifted beachrock
Longshore drift
(prevailing)
Uplifted marine
notch

Figure 4

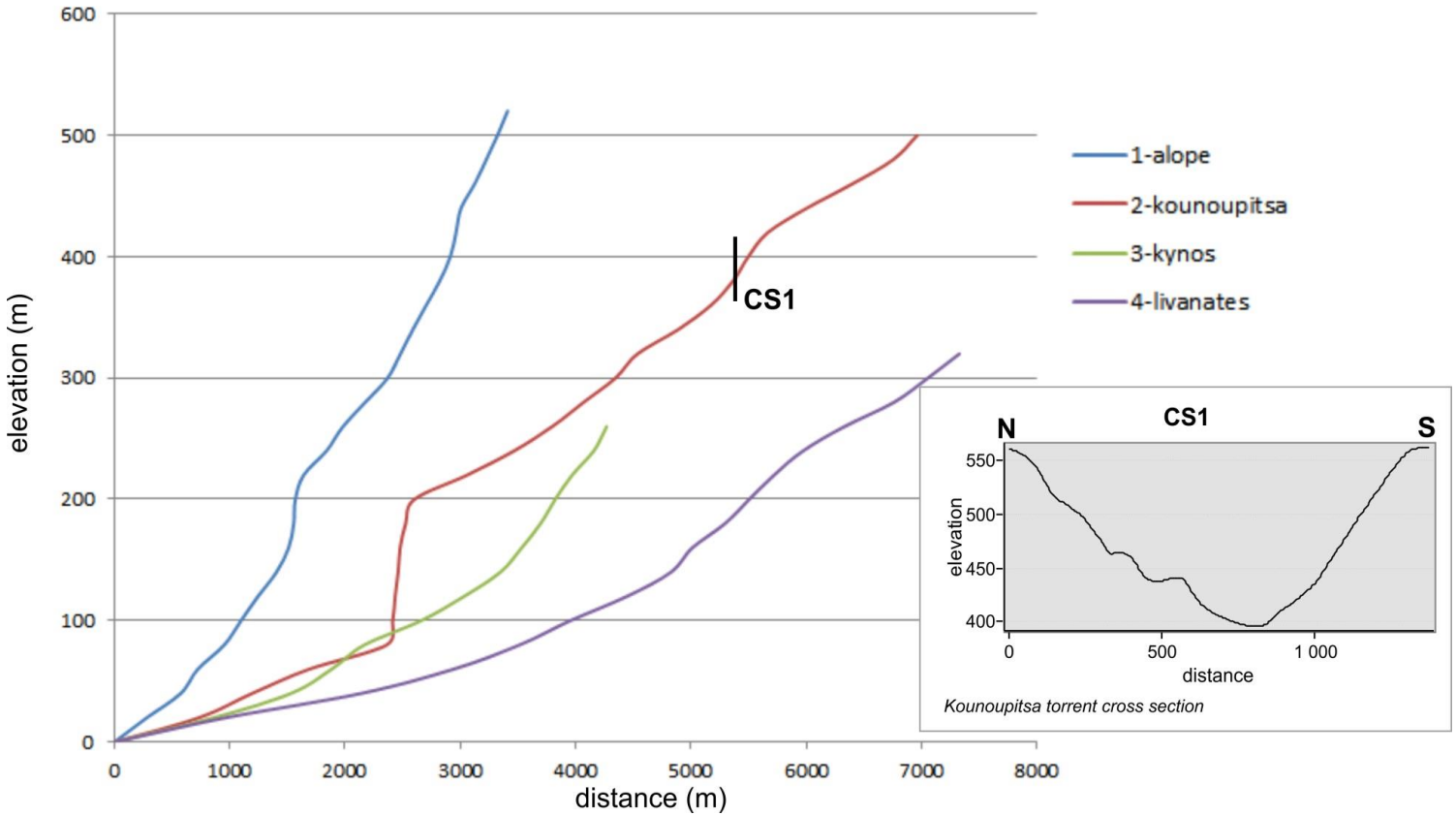
600
500
400
300
200
100
0
elevation (m)
0
1000
2000
3000
4000
5000
6000
7000
8000
distance (m)
CS1
1-alope
2-kounoupitsa
3-kynos
4-livanates
N
CS1
S
550
500
450
400
elevation
0
500
1 000
distance
Kounoupitsa torrent cross section

Figure 5

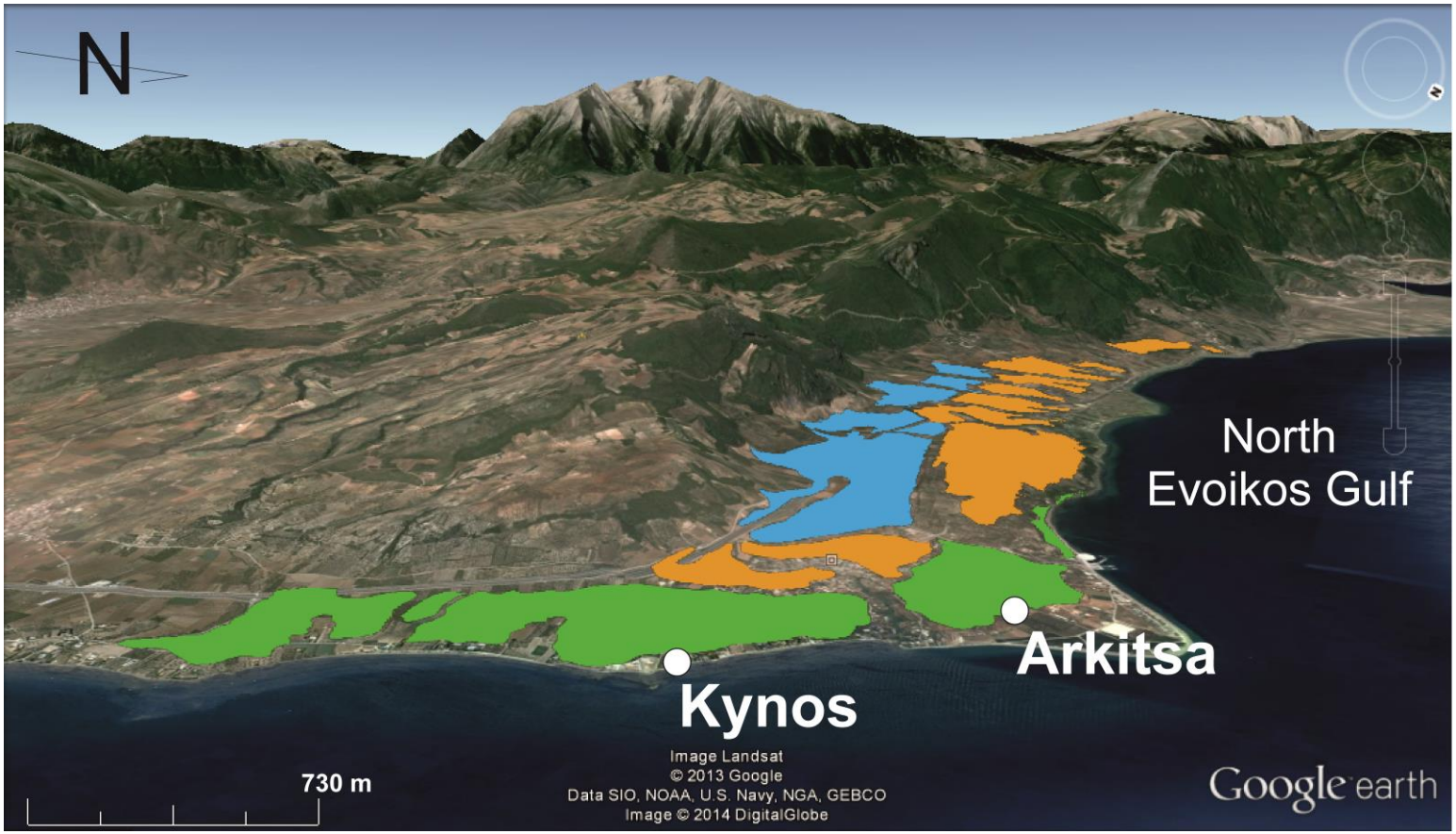
N
North
Evoikos Gulf
Arkitsa
Kynos
730 m
Image Landsat
© 2013 Google
Data SIO, NOAA, U.S. Navy, NGA, GEBCO
Image © 2014 DigitalGlobe
Google earth

Figure 6

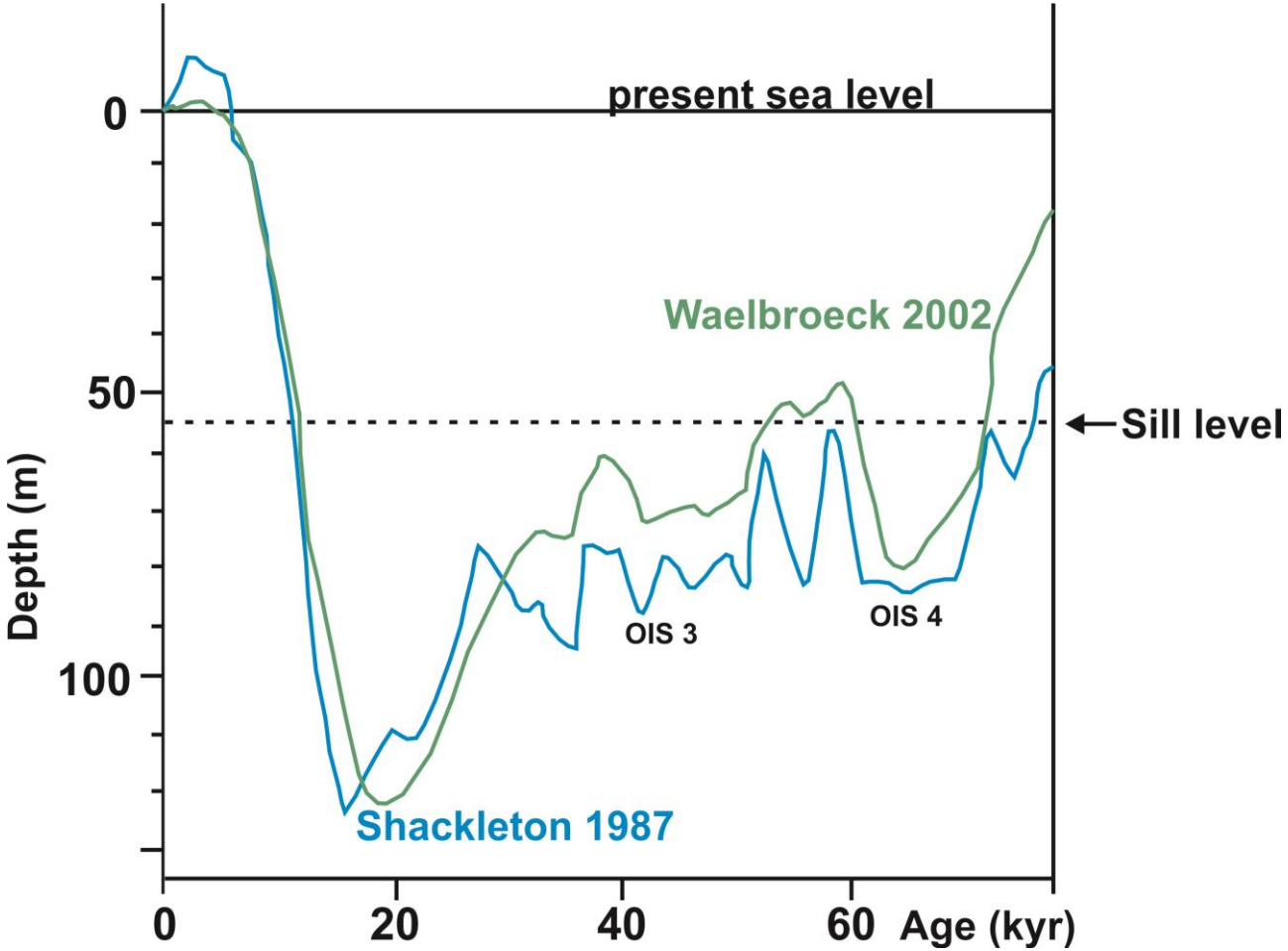
present sea level
0
50
100
Depth (m)
Waelbroeck 2002
Sill level
OIS 3
OIS 4
Shackleton 1987
0
20
40
60
Age (kyr)

Plate 1

Plate 2